Journal of Chromatography B 1077–1078 (2018) 71–76

Contents lists available at ScienceDirect

Journal of Chromatography B

journal homepage: www.elsevier.com/locate/jchromb

Serum metabolite profiling of cutaneous T-cell lymphoma based on a multiplatform approach

Guoting Jiang[a,1], Xiaoyan Shen[b,1], Hongyan Kang[a], Kejia Li[b], Jie Zheng[b,*], Yunqiu Yu[a,*]

[a] School of Pharmacy, Fudan University, Shanghai 201203, PR China
[b] Department of Dermatology, Ruijin Hospital, Shanghai Jiaotong University School of Medicine, Shanghai 200025, PR China

ARTICLE INFO

Keywords:
Multiplatform
Metabolomics
Cutaneous T-cell lymphoma
Differential metabolites

ABSTRACT

Cutaneous T-cell lymphoma (CTCL) is a class of non-Hodgkin lymphoma with a difficult early diagnosis. The overall annual age-adjusted incidence of CTCL had consistently increased to around 10.2 cases per million persons. However, our knowledge regarding its mechanism of disease origin and progression remains unclear. In this study, serum samples from 31 CTCL patients and 31 matched healthy volunteers were analyzed in depth to screen metabolites capable of differentiating CTCL from controls. To obtain a higher coverage of metabolome with various hydrophilicity, a multiplatform approach with GC–MS and UHPLC-QTOF-MS has been employed. Data were analyzed by multivariate statistical analysis and CTCL group was separated from control group successfully using supervised OPLS-DA model. A total of 51 CTCL-regulated metabolites were identified, among which 15 differential metabolites have an AUC > 0.9 in receiver operating characteristic (ROC) curve analysis. Glycerophospholipid metabolism, tryptophan metabolism and purine metabolism were highlighted as 3 major altered pathways in CTCL serum. These alterations revealed impacts to membrane stability and weakened immune as well as ATP depletion associated with CTCL. Overall, these results aid in improving understanding of the mechanism related to CTCL, and demonstrate this multiplatform approach is suitable for serum metabolomics researches.

1. Introduction

Cutaneous T-cell lymphoma (CTCL) is a heterogeneous group of extranodal non-Hodgkin's lymphomas characterized by clonal expansion of skin-invasive T cells [1]. World Health Organization (WHO) and European Organization for Research and Treatment of Cancer (EORTC) published a consensus classification (WHO-EORTC) for primary CTCL in 2005 [2]. Mycosis fungoides (MF) is the most common diagnosis of CTCL, representing 44–62% of cases [3], which has an indolent clinical course initiating as patches and plaques for years and eventually forming tumors. The overall annual age-adjusted incidence of CTCL consistently increased since the early 1970s, but has stabilized in recent years at around 10.2 cases per million persons [4]. Despite advances in immunohistochemistry and molecular methodology, early diagnosis of CTCL is still difficult, partly because of its phenotypic overlap with benign inflammatory skin diseases [5,6]. It takes 48 months on average to make a definite diagnosis after the first development of skin lesions [7]. In recent decades, there are many studies focus on CTCL pathogenesis, but the mechanism of disease origin and progression is still unclear [8–10]. Therefore, biomarkers screening and mechanism study make much sense to early diagnosis and effective treatment for CTCL.

With the enhancement in detection sensitivity and high-throughput capacity, “omics” techniques have been extensively utilized in disease research. Previous genomics study implicates mutations in 17 genes in CTCL pathogenesis [11]. It was found that transcriptomics and proteomics can be used to assist CTCL diagnosis and classification [12,13]. Metabolomics, the youngest sibling in ‘omics’ field, plays an important role in systems biology due to the ability to provide comprehensive analysis of all metabolites (molecules < 1 kDa) present in biofluid samples [14,15]. Metabolomics always indicates alterations in upstream gene and protein expression, and has been widely used in the research of diagnosing pathology and biomarker screening [16–18]. Our previous UHPLC-QTOF-MS based metabolomics study has found 36 differential metabolites in CTCL plasma, among which 4 compounds were identified by reference standards [19]. In this research, we employed a multiplatform approach to further investigate the metabolite profiling alteration in CTCL serum samples, with no additional anticoagulants which may interfere the metabolome constituent measurement and dilute samples by drawing water out of cells [20]. It is well accepted that no single platform is able to detect the entire

* Corresponding authors.
E-mail addresses: jie-zheng2001@126.com (J. Zheng), yqyu@shmu.edu.cn (Y. Yu).
[1] These authors contributed equally to this work.

https://doi.org/10.1016/j.jchromb.2018.01.034
Received 1 June 2017; Received in revised form 7 December 2017; Accepted 26 January 2018
Available online 31 January 2018
1570-0232/

metabolome, therefore multiplatform approaches are usually employed in untargeted metabolomics studies. With the combined use of two complementary platforms, GC–MS and UHPLC-QTOF-MS, a higher coverage of metabolome was achieved, making the global metabolite profiling more meaningful and reliable.

2. Materials and methods

2.1. Chemicals and reagents

Methanol (HPLC Grade) was obtained from Sinopharm Chemical Reagent Co., Ltd. (Shanghai, China). Acetonitrile (HPLC Grade) and Formic Acid (HPLC Grade) were purchased from Dikma Technologies Inc. (Lake Forest, CA, USA). Tridecanoic acid, pyridine (HPLC grade), methoxyamine hydrochloride, MSTFA (*N*-Methyl-*N*-(trimethylsilyl) trifluoroacetamide) and TMCS (chlorotrimethylsilane) were purchased from Sigma-Aldrich (St. Louis, MO, USA).

2.2. Sample collection

The present prospective study was approved by the Ethics Committee of Ruijin Hospital, Shanghai Jiaotong University School of Medicine, and informed consent was obtained from all participants. CTCL serum samples were collected from 31 patients and serum samples from age- and sex-matched healthy volunteers (Table 1) were used as controls. For serum collection, whole blood was collected and left standing at room temperature for 1 h to clot before centrifugation for 10 min at 3000 rpm. All serum samples were immediately aliquoted and stored at −80 °C until further analysis.

2.3. Sample preparation for GC–MS analysis

After thawing at room temperature, 50 μL of serum from each sample was pipetted into Eppendorf tubes. Next, 200 μL of −20 °C methanol (containing 40 μg/mL tridecanoic acid as internal standard) was added to each sample, and the mixture was vortexed for 5 min and left standing at room temperature for 10 min to precipitate proteins completely. After centrifugation at 12,000 rpm for 10 min, 180 μL supernatant was collected and transferred for drying under a nitrogen stream at 40 °C. Then, dried samples were dissolved in 50 μL of pyridine (containing 15 mg/mL of methoxyamine hydrochloride), and the oximation reaction was conducted at 40 °C for 2 h, followed by silylation reaction with 40 μL of MSTFA (containing 1% TMCS) at 40 °C for 1 h. After centrifugation at 12,000 rpm for 10 min, 20 μL of the supernatant was collected and pooled to prepare the quality control (QC) samples for GC–MS analysis.

2.4. GC–MS analysis

GC–MS analysis of derivatized samples was executed with a 7890B gas chromatograph, fitted with a 7693 autosampler and coupled to a 5977A quadrupole mass analyzer (Agilent, Santa Clara, CA, USA) in full scan mode. Chromatographic separations of metabolites were accomplished on a DB-5 MS fused silica capillary column (30 m × 250 μm × 0.25 μm, Agilent, USA). The carrier gas, helium, was operated at a flow rate of 1.2 mL/min and temperatures of inlet, interface and ion source were set at 300 °C, 280 °C and 230 °C, respectively. The injection volume and split ratio were set to 1 μL and 2:1. The GC oven temperature program was set as follows: initiated at 70 °C, kept for 3 min, then ramped at 5 °C/min up to 300 °C and finally held for 5 min. The electron impact (70 eV) was applied as the ionization mode and gain factor was set at 2.0. The mass signal acquisition (33–600, *m/z*) was performed after 6.0 min of solvent delay by MassHunter Acquisition Software (Agilent, USA). Samples of different groups were processed randomly.

Table 1
Demographics information of the study cohorts.

Sample type	Items	Control	CTCL
Serum	Female/male	13/18	13/18
	Age (years)	53.9 ± 13.9	54.6 ± 14.6
	Duration (years)	NA	4.3 ± 4.2

Values are reported as the mean ± SD. There is no duration for the control group (NA). *p* value > 0.05 for *t*-test for the age between control and CTCL subjects.

2.5. UHPLC-QTOF-MS analysis

After process described in sample preparation for GC–MS analysis until protein precipitation, supernatant was collected and analyzed by UHPLC-QTOF-MS directly, rather than drying and derivatization. QC samples were composed of the supernatant of all samples equally and analyzed at an interval of 10 samples to verify reproducibility of the analysis. Then, a 5 μL aliquot of the supernatant was injected into a 1260 Infinity UHPLC system (Agilent, USA) equipped an ACQUITY UPLC HSS T3 column (2.1 × 100 mm, 1.8 μm, Waters, USA) at a constant column temperature of 35 °C for chromatographic separation. The flow rate was 0.3 mL/min and the mobile phase were (A) H_2O with 0.1% formic acid and (B) acetonitrile. The programmed gradient was set as follows: 0 min, 98% A; 2 min, 98% A; 12 min, 5% A; 22 min, 5% A with a 5 min post run at initial ratio.

The eluted metabolites were analyzed by a 6520 QTOF-MS (Agilent, USA) in positive and negative electrospray ionizations with a full-scan range from 50 to 1000 *m/z*, and data were collected in centroid mode. Nitrogen was used as desolvation gas at a flow rate of 10 L/min at 350 °C. The capillary voltage and nebulizer pressure were set at 3.5 kV and 40 psi, respectively. All samples were run in a random sequence.

2.6. Data processing

Raw data were converted to mzData format by Agilent MassHunter Qualitative Analysis software, then uploaded to XCMS online (https://xcmsonline.scripps.edu) [21] for peak alignment, retention time correction and relative quantification of metabolite profiling. A two dimensional data table of metabolite features (retention time and *m/z*) and their peak areas were generated. Afterwards, the peak areas were normalized and “80% rule” [22] was employed for the peak filtering. Multivariate data analysis was performed using SIMCA 13 (Umetrics, Sweden). An unsupervised model, principal components analysis (PCA), was first performed to visualize the discrimination between the control group and CTCL group based on serum metabolites, followed by supervised models including partial least squares discriminant analysis (PLS-DA) and orthogonal partial least squares discriminant analysis (OPLS-DA) to enhance separation and screening differential metabolites. Furthermore, 200 times of permutation test cross validation was performed to ensure the suitability of the model.

The differential metabolites were screened according to strict criteria: (1) VIP value larger than 1.0 constructed from the OPLS-DA; (2) *p* value of *t*-test smaller than 0.05; (3) fold changes (FC) larger than 1.5. Next, the discriminating metabolites screened from GC–MS data were identified by combining NIST database and the Human Metabolome Database (HMDB, http://www.hmdb.ca) [23]. Metabolites identification of UHPLC-QTOF-MS was executed by searching HMDB and METLIN (https://metlin.scripps.edu) [24] based on the accurate mass number with a mass error within 20 ppm. Furthermore, some metabolites were further confirmed by comparing with reference standards. Heatmap employing GraphPad was carried out to visualize the metabolic alterations of the remarkable shifts metabolites. The receiver operating characteristic (ROC) curves were constructed to evaluate the sensitivity and specificity of these differential metabolites with Medcalc software. Metabolic pathway analysis was performed by MetaboAnalyst

(http://www.metaboanalyst.ca/) [25] based on the database sources including KEGG, HMDB, and so on, to identify the affected metabolic pathways and facilitate further biological interpretation.

3. Results

3.1. Multivariate statistical analysis

A RSD of 20% could cover over 80% features in QC analysis of all three analysis methods (Fig. S1), which indicated that the present methods had good repeatability and the acquired data are robust and worth further study [26]. PCA was initially utilized to visualize general clustering trends among the observations. Although there were overlaps between the control and CTCL group, tendencies of separation were appeared in the score plots (Fig. S2a, b and c). A supervised PLS-DA model was used to exhibit the metabolic distinction. The PLS-DA scores plots presented obviously separations of healthy controls and CTCL patients from metabolic profiling (Fig. S2d, e and f). In permutation test, models are considered valid for their ability to describe variation and predict group membership when y intercept of R2 is < 0.3–0.4 and y intercept of Q2 is < 0.05, respectively [27]. The parameters obtained from 200 times permutation test met the validation criteria (Fig. S2g, h and i), indicating that the PLS-DA models was not over-fitted and had reliable predictive ability. A supervised OPLS-DA model was further constructed to present the metabolic difference between these two groups (Fig. 1), and provided VIP values for differential metabolites screening.

3.2. Differential metabolites identification

Based on VIP values of features in the OPLS-DA model, p value of t-test and FC, a set of remarkable features (VIP ≥ 1, $p \leq 0.05$ and FC ≥ 1.5) were selected. After identification with the metabolite databases, 8, 37 and 10 metabolites were annotated in the GC–MS, UHPLC-QTOF-MS positive and negative ion modes (Tables S1, S2), respectively. Among these, 4 GC-metabolites and 5 LC-metabolites were confirmed by the reference standards. It was also noted that 4 differential compounds were detected by two methods, and therefore there were 51 differential metabolites (Fig. S3).

The contrast of differential metabolites between the control and CTCL group were visualized in a heatmap plot (Fig. 2). The ratio of metabolites in CTCL to average of those in healthy control samples were first calculated, and then the metabolic alterations were demonstrated as log10 (ratio). The heatmap was plotted in a green-red color scale

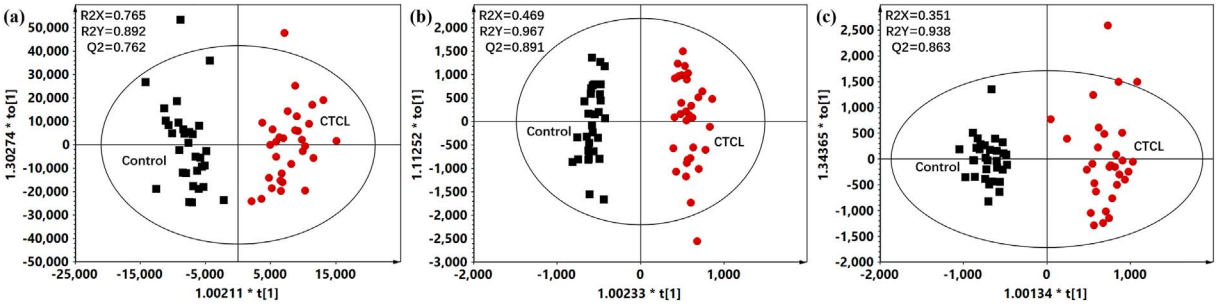

Fig. 1. OPLS-DA scores plots for GC–MS (a), UHPLC-QTOF-POS (b), UHPLC-QTOF-NEG (c) data.

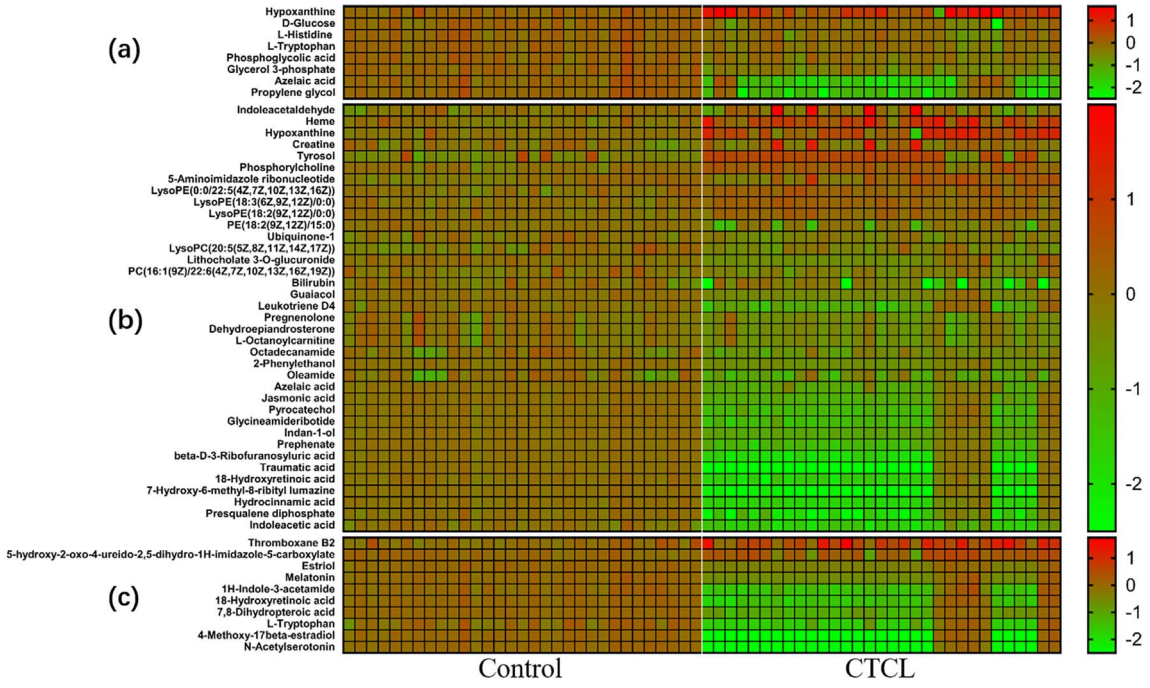

Fig. 2. Heatmap of identified metabolites analyzed using GC–MS (a), UHPLC-QTOF-POS (b) and UHPLC-QTOF-NEG (c). The heatmap was plotted in a green-red color scale with red indicating an increase and green indicating a decrease of metabolite level. (For interpretation of the references to color in this figure legend, the reader is referred to the web version of this article.)

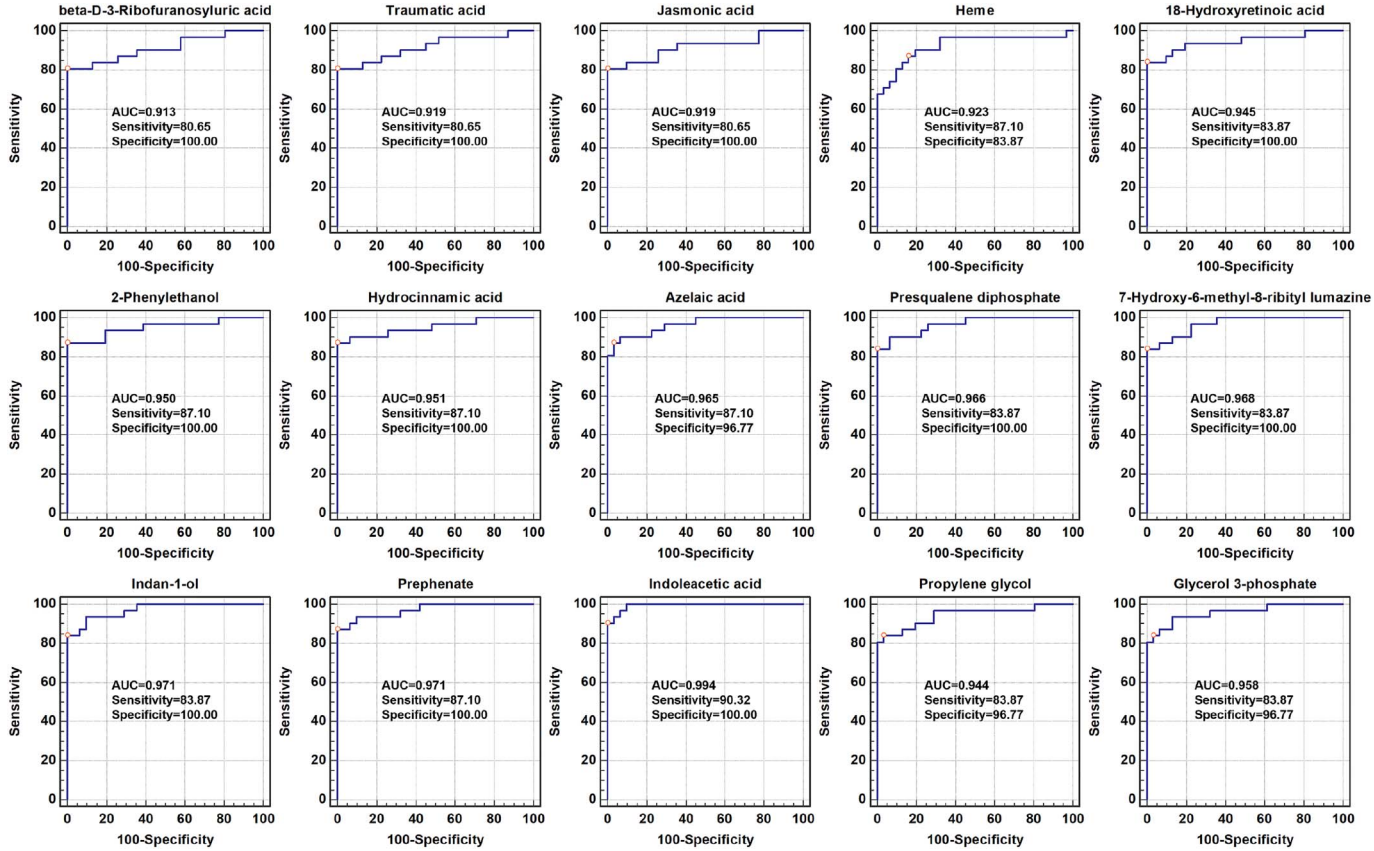

Fig. 3. The typical ROC curve plots of differential metabolites with AUC values > 0.9.

with red indicating an increase and green indicating a decrease of metabolite level.

3.3. Receiver operating characteristic curve

ROC curve analysis is generally considered to be the standard method for biomarker performance assessment [28]. All 51 differential metabolites identified were analyzed by ROC curve. The ROC curve analysis results showed that the area under the curve (AUC) of 2 and 13 metabolites were > 0.9 in GC–MS and UHPLC-QTOF-MS positive mode (Fig. 3), respectively, which means high-performance prediction was readily achieved.

3.4. Metabolic pathway analysis

The HMDB IDs of 51 differential metabolites were imported into the MetaboAnalyst 3.0, and 3 metabolic pathways with a p value < 0.05 were generated by the web-based software, which were supposed to be significantly altered in CTCL patients and may serve as potential therapeutic targets. These 3 pathways were characterized as (a) glycerophospholipid metabolism, (b) tryptophan metabolism and (c) purine metabolism (Fig. 4).

4. Discussion

CTCL is a class of non-Hodgkin lymphoma caused by a mutation of T cells, which is a type of cancer of the immune system. The early diagnosis and effective treatment for CTCL are still difficult as it has phenotypic overlap with benign inflammatory skin diseases and the mechanism of disease origin and progression is still unclear. In this study, we investigated the metabolite profiling alteration in CTCL serum samples using GC–MS combined UHPLC-QTOF-MS analysis. A total of 51 CTCL-regulated metabolites were identified involved in 3 pathways. Compared with our previous study [19], the combination of two complementary analysis platforms had greatly increased the metabolome coverage and much stricter criteria were adopted in differential metabolites screening.

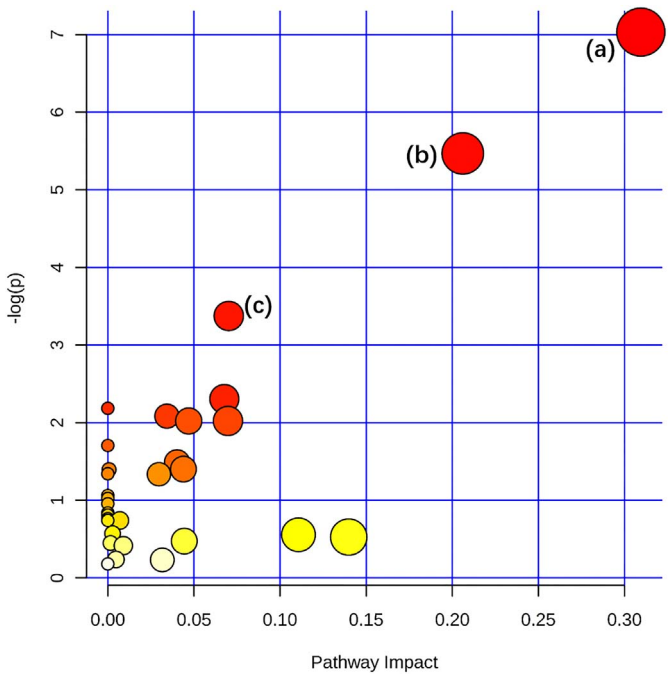

Fig. 4. A systemic view of altered metabolic pathways that associate with the CTCL group in this study. (a) Glycerophospholipid metabolism, (b) tryptophan metabolism and (c) purine metabolism had a p value < 0.05.

Proliferation of tumor cells requires a continuous supply of phospholipid content for synthesis and maintenance of membrane integrity as well as protein modifications [29,30]. The abnormal proliferation of malignant T cells in CTCL is similar to the infinite reproduction of tumor cells. Changes in glycerophospholipid metabolism suggest membrane degradation or morphological changes in proliferation of malignant T cells because of its important role in maintaining cell membrane integrity. LysoPE(18:3/0:0), LysoPE(18:2/0:0), LysoPE(0:0/22:5) and phosphorylcholine showed significant increases in CTCL serum, while abundances of LysoPC(20:5), PC(16:1/22:6) and PE(18:2/15:0) decreased. These inconsistent trends might be caused by membrane instability and the subsequent attempt of malignant T cells to repair them [31].

The pathway analysis showed an abnormality in the tryptophan metabolism, and the levels of tryptophan, indoleacetic acid, melatonin, *N*-Acetylserotonin and 1H-Indole-3-acetamide in serum were all reduced. Tryptophan plays a pivotal role in the immune system, and elevated tryptophan consumption helps tumors to overcome immune barriers to cancer progression [32]. A most recent study pointed out that expression of two tryptophan-catabolizing enzymes, indoleamine 2,3-deoxygenase 1 (IDO1) and tryptophan 2,3-dioxygenase (TDO), was upregulated in CTCL [33], which would increase the consumption of tryptophan. It could be concluded that overall decrease in the tryptophan metabolism pathway shown in our results is due to the upregulated of tryptophan-catabolizing enzymes and contributes to the CTCL disease progression.

Purine metabolism disorders have been associated with many types of cancers, such as lung cancer [34], liver cancer [35], prostate cancer [36] and so on. Hypoxanthine is a naturally occurring purine derivative and a key intermediate in purine metabolism. It was detected in both GC–MS and UHPLC-QTOF-MS positive mode. It had a significant increase in CTCL serum (8.14–9.52 folds), consistent with our previous studies of plasma metabolomics. The sharply upregulated hypoxanthine means an increased ATP depletion occurred, since the purine nucleotide ATP is the energy currency of the cell and hypoxanthine is the extracellular compound most directly related to intracellular ATP [37].

5. Conclusion

An untargeted multiplatform approach was applied to provide further insight into the metabolite profiling regulations and discover differential metabolites for CTCL serum samples. After multivariate analysis, 51 CTCL-regulated metabolites were identified. The result of metabolic pathway analysis highlighted glycerophospholipid metabolism, tryptophan metabolism and purine metabolism as 3 major altered pathways in CTCL serum. These alterations impact membrane stability and weakened immune as well as ATP depletion. It could be concluded that serum metabolites are sensitively and specificity responsive to people's health condition and these differential metabolites may be applied for the diagnosis and prediction for CTCL. The combination of GC–MS and UHPLC-QTOF-MS had greatly increased the metabolome coverage and validated the result of each other, and it's a useful tool for better understanding the metabolic changes in serum samples.

Acknowledgements

This study was funded by a grant from the National Science Foundation Project of China (KRF301100).

Appendix A. Supplementary data

Supplementary data to this article can be found online at https://doi.org/10.1016/j.jchromb.2018.01.034.

References

[1] E.J. Kim, S. Hess, S.K. Richardson, S. Newton, L.C. Showe, B.M. Benoit, R. Ubriani, C.C. Vittorio, J.M. Junkins-Hopkins, M. Wysocka, A.H. Rook, Immunopathogenesis and therapy of cutaneous T cell lymphoma, J. Clin. Invest. 115 (2005) 798–812.
[2] R. Willemze, E.S. Jaffe, G. Burg, L. Cerroni, E. Berti, S.H. Swerdlow, E. Ralfkiaer, S. Chimenti, J.L. Diaz-Perez, L.M. Duncan, F. Grange, N.L. Harris, W. Kempf, H. Kerl, M. Kurrer, R. Knobler, N. Pimpinelli, C. Sander, M. Santucci, W. Sterry, M.H. Vermeer, J. Wechsler, S. Whittaker, C.J. Meijer, WHO-EORTC classification for cutaneous lymphomas, Blood 105 (2005) 3768–3785.
[3] Y. Eklund, A. Aronsson, A. Schmidtchen, T. Relander, Mycosis fungoides: a retrospective study of 44 Swedish cases, Acta Derm. Venereol. 96 (2016) 669–673.
[4] K. Korgavkar, M. Xiong, M. Weinstock, Changing incidence trends of cutaneous T-cell lymphoma, JAMA Dermatol. 149 (2013) 1295.
[5] K.G. Sidiropoulos, M.E. Martinez-Escala, O. Yelamos, J. Guitart, M. Sidiropoulos, Primary cutaneous T-cell lymphomas: a review, J. Clin. Pathol. 68 (2015) 1003–1010.
[6] I.R. Kirsch, R. Watanabe, J.T. O'Malley, D.W. Williamson, L.L. Scott, C.P. Elco, J.E. Teague, A. Gehad, E.L. Lowry, N.R. LeBoeuf, J.G. Krueger, H.S. Robins, T.S. Kupper, R.A. Clark, TCR sequencing facilitates diagnosis and identifies mature T cells as the cell of origin in CTCL, Sci. Transl. Med. 7 (2015) (308ra158).
[7] R. van Doorn, C.W. Van Haselen, P.C.V. Vader, M.L. Geerts, F. Heule, M. de Rie, P.M. Steijlen, S.K. Dekker, W.A. van Vloten, R. Willemze, Mycosis fungoides - disease evolution and prognosis of 309 Dutch patients, Arch. Dermatol. 136 (2000) 504–510.
[8] Y. Nahidi, N.T. Meibodi, K. Ghazvini, H. Esmaily, M. Hesamifard, Evaluation of the association between Epstein-Barr virus and mycosis fungoides, Indian J. Dermatol. 60 (2015) 321.
[9] J. Maj, A.M. Jankowska-Konsur, A. Halon, Z. Wozniak, E. Plomer-Niezgoda, A. Reich, Expression of CXCR4 and CXCL12 and their correlations to the cell proliferation and angiogenesis in mycosis fungoides, Postep. Dermatol. Alergol. 32 (2015) 437–442.
[10] E. Lebas, F. Libon, A.F. Nikkels, Koebner phenomenon and mycosis fungoides, Case Rep. Dermatol. 7 (2015) 287–291.
[11] J. Choi, G. Goh, T. Walradt, B.S. Hong, C.G. Bunick, K. Chen, R.D. Bjornson, Y. Maman, T. Wang, J. Tordoff, K. Carlson, J.D. Overton, K.J. Liu, J.M. Lewis, L. Devine, L. Barbarotta, F.M. Foss, A. Subtil, E.C. Vonderheid, R.L. Edelson, D.G. Schatz, T.J. Boggon, M. Girardi, R.P. Lifton, Genomic landscape of cutaneous T cell lymphoma, Nat. Genet. 47 (2015) 1011–1019.
[12] I.V. Litvinov, E. Netchiporouk, B. Cordeiro, M.A. Dore, L. Moreau, K. Pehr, M. Gilbert, Y. Zhou, D. Sasseville, T.S. Kupper, The use of transcriptional profiling to improve personalized diagnosis and management of cutaneous T-cell lymphoma (CTCL), Clin. Cancer Res. 21 (2015) 2820–2829.
[13] C.W. Liu, N. Shea, S. Rucker, L. Harvey, P. Russo, R. Saul, M.F. Lopez, A. Mikulskis, S. Kuzdzal, E. Golenko, D. Fishman, E. Vonderheid, S. Booher, E.W. Cowen, S.T. Hwang, G.R. Whiteley, Proteomic patterns for classification of ovarian cancer and CTCL serum samples utilizing peak pairs indicative of post-translational modifications, Proteomics 7 (2007) 4045–4052.
[14] O. Fiehn, Metabolomics - the link between genotypes and phenotypes, Plant Mol. Biol. 48 (2002) 155–171.
[15] G.J. Patti, O. Yanes, G. Siuzdak, Innovation: metabolomics: the apogee of the omics trilogy, Nat. Rev. Mol. Cell Biol. 13 (2012) 263–269.
[16] G.D. Lewis, A. Asnani, R.E. Gerszten, Application of metabolomics to cardiovascular biomarker and pathway discovery, J. Am. Coll. Cardiol. 52 (2008) 117–123.
[17] A.H. Zhang, H. Sun, X.J. Wang, Recent advances in metabolomics in neurological disease, and future perspectives, Anal. Bioanal. Chem. 405 (2013) 8143–8150.
[18] E.G. Armitage, C. Barbas, Metabolomics in cancer biomarker discovery: current trends and future perspectives, J. Pharm. Biomed. Anal. 87 (2014) 1–11.
[19] Q.Y. Zhou, Y.L. Wang, X. Li, X.Y. Shen, K.J. Li, J. Zheng, Y.Q. Yu, Metabolomics investigation of cutaneous T cell lymphoma based on UHPLC-QTOF/MS, Asian Pac. J. Cancer Prev. 15 (2014) 5417–5421.
[20] A. Kwasnik, C. Tonry, A.M. Ardle, A.Q. Butt, R. Inzitari, S.R. Pennington, Proteomes, their compositions and their sources, Adv. Exp. Med. Biol. 919 (2016) 3–21.
[21] R. Tautenhahn, G.J. Patti, D. Rinehart, G. Siuzdak, XCMS online: a web-based platform to process untargeted metabolomic data, Anal. Chem. 84 (2012) 5035–5039.
[22] A.K. Smilde, M.J. van der Werf, S. Bijlsma, B.J. van der Werff-van der Vat, R.H. Jellema, Fusion of mass spectrometry-based metabolomics data, Anal. Chem. 77 (2005) 6729–6736.
[23] D.S. Wishart, T. Jewison, A.C. Guo, M. Wilson, C. Knox, Y. Liu, Y. Djoumbou, R. Mandal, F. Aziat, E. Dong, S. Bouatra, I. Sinelnikov, D. Arndt, J. Xia, P. Liu, F. Yallou, T. Bjorndahl, R. Perez-Pineiro, R. Eisner, F. Allen, V. Neveu, R. Greiner, A. Scalbert, HMDB 3.0-the human metabolome database in 2013, Nucleic Acids Res. 41 (2012) D801–D807.
[24] C.A. Smith, G. O'Maille, E.J. Want, C. Qin, S.A. Trauger, T.R. Brandon, D.E. Custodio, R. Abagyan, G. Siuzdak, METLIN - a metabolite mass spectral database, Ther. Drug Monit. 27 (2005) 747–751.
[25] J. Xia, I.V. Sinelnikov, B. Han, D.S. Wishart, MetaboAnalyst 3.0-making metabolomics more meaningful, Nucleic Acids Res. 43 (2015) W251–W257.
[26] G. Jiang, H. Kang, Y. Yu, Cross-platform metabolomics investigating the intracellular metabolic alterations of HaCaT cells exposed to phenanthrene, J. Chromatogr. B 1060 (2017) 15–21.
[27] U. Paolucci, K.E. Vigneau-Callahan, H. Shi, W.R. Matson, B.S. Kristal, Development of biomarkers based on diet-dependent metabolic serotypes: characteristics of

component-based models of metabolic serotypes, OMICS 8 (2004) 221–238.
[28] J. Xia, D.I. Broadhurst, M. Wilson, D.S. Wishart, Translational biomarker discovery in clinical metabolomics: an introductory tutorial, Metabolomics 9 (2013) 280–299.
[29] B. Szachowicz-Petelska, I. Dobrzynska, S. Sulkowski, Z. Figaszewski, Characterization of the cell membrane during cancer transformation, J. Environ. Biol. 31 (2010) 845–850.
[30] C.M. Spickett, K. Tveen-Jensen, A. Reis, A.R. Pitt, Protein modification and phospholipid oxidation, Free Radic. Biol. Med. 65 (2013) S15.
[31] C.M. Jones, M.E. Monge, J. Kim, M.M. Matzuk, F.M. Fernandez, Metabolomic serum profiling detects early-stage high-grade serous ovarian cancer in a mouse model, J. Proteome Res. 14 (2015) 917–927.
[32] G.C. Prendergast, Cancer: why tumours eat tryptophan, Nature 478 (2011) 192–194.
[33] P. Maliniemi, K. Laukkanen, L. Vakeva, K. Dettmer, T. Lipsanen, L. Jeskanen, A. Bessede, P.J. Oefner, M.E. Kadin, A. Ranki, Biological and clinical significance of tryptophan-catabolizing enzymes in cutaneous T-cell lymphomas, OncoImmunology 6 (2017) e1273310.
[34] M.T. Goswami, G. Chen, B.V. Chakravarthi, S.S. Pathi, S.K. Anand, S.L. Carskadon, T.J. Giordano, A.M. Chinnaiyan, D.G. Thomas, N. Palanisamy, D.G. Beer, S. Varambally, Role and regulation of coordinately expressed de novo purine biosynthetic enzymes PPAT and PAICS in lung cancer, Oncotarget 6 (2015) 23445–23461.
[35] Y. Shao, B. Zhu, R. Zheng, X. Zhao, P. Yin, X. Lu, B. Jiao, G. Xu, Z. Yao, Development of urinary pseudotargeted LC-MS-based metabolomics method and its application in hepatocellular carcinoma biomarker discovery, J. Proteome Res. 14 (2015) 906–916.
[36] W. Struck-Lewicka, M. Kordalewska, R. Bujak, A. Yumba Mpanga, M. Markuszewski, J. Jacyna, M. Matuszewski, R. Kaliszan, M.J. Markuszewski, Urine metabolic fingerprinting using LC-MS and GC–MS reveals metabolite changes in prostate cancer: a pilot study, J. Pharm. Biomed. Anal. 111 (2015) 351–361.
[37] R.A. Harkness, Hypoxanthine, xanthine and uridine in body fluids, indicators of ATP depletion, J. Chromatogr. 429 (1988) 255–278.